MEASUREMENT OF FINE SCALE STRUCTURE IN TURBULENCE BY TIME-RESOLVED DUAL-PLANE STEREOSCOPIC PIV

Mamoru Tanahashi, Tetsu Hirayama, Shohei Taka, Toshio Miyauchi
Department of Mechanical and Aerospace Engineering,
Tokyo Institute of Technology
2-12-1 Ookayama, Meguro-ku, Tokyo 152-8850, Japan
mtanahas@mes.titech.ac.jp, hirayama@navier.mes.titech.ac.jp
shtaka@navier.mes.titech.ac.jp, tmiyauch@mes.titech.ac.jp

ABSTRACT

To investigate fine scale structure of turbulent flows, time-resolved dual-plane stereoscopic particle image velocimetry (TRDPSPIV) has been developed using high-repetition-rate Nd:YAG lasers for industrial processing and high-speed CMOS cameras. This system provides all three velocity components and nine velocity gradients with high spatial and temporal resolution. The developed system was applied to velocity measurements of a turbulent jet, and the velocities obtained in both planes showed very similar pattern because of the small distance between the planes. It is shown that probability density functions of the measured nine velocity gradients agree well with those obtained from direct numerical simulation (DNS). From these velocity gradients, various flow properties such as vorticity vectors, second invariant of velocity gradient tensor and energy dissipation rate are obtained exactly. These properties allow an eddy identification, which has been used in the analysis of DNS, to investigate fine scale structure of turbulence. Velocity distributions around the experimentally-detected fine scale eddies have an elliptic feature, and the histograms of the diameter and maximum azimuthal velocity of the detected eddy show peaks at $D/\eta \approx 10$ and $u_{\theta,max}/u_k \approx 0.75$. These characteristics of the fine scale eddy coincide with those obtained from DNS.

INTRODUCTION

In our previous studies on fine scale structure of turbulence by direct numerical simulation (DNS) (Tanahashi et al., 1997; 2001; 2004b), the existence of universal fine scale structure (coherent fine scale structure), which is independent on Reynolds number and type of flow field, have been revealed. The diameter and the maximum azimuthal velocity of coherent fine scale eddies can be scaled by Kolmogorov length (η) and Kolmogorov velocity (u_k). Except for near wall turbulence (Tanahashi et al., 2004b), the most expected diameter and maximum azimuthal velocity are 8η and $1.2u_k$. It should be noted that the azimuthal velocity of intense fine scale eddies reaches $3 \sim 4u'_{rms}$. Coherent fine scale eddies have strong three dimensional characteristics and are moving with velocity of the order of u'_{rms} (Tanahashi et al., 1999). To investigate these fine scale structure experimentally, simultaneous measurement of three velocity components and nine velocity gradients is needed.

Particle image velocimetry (PIV), which gives instantaneous maps of the velocity field, is a useful, firmly established, non-intrusive measurement technique. To apply this PIV measurement to various industrial purposes as well as to fundamental research, many research groups have explored extensively over the past decade. To investigate temporal sequence of turbulent flows, high temporal resolution has been required as well as high spatial resolution. The combination of PIV and high speed photography was conducted to track an unsteady fluid flow (Vogel and Lauterborn, 1988), whereas the use of the light scattering in the forward direction limited the spatial resolution. To record the time evolution of the gas velocity field and the flame boundary, a cinema PIV technique was used for turbulent combustion (Upatnieks et al., 2002). Image reproduction from movie camera to CCD camera is necessary to obtain vector maps for this cinema PIV. Recently, high-speed acquisition PIV with several hundreds Hz has become possible with a development of high speed CCD and CMOS cameras, and several high-repetition-rate double-pulsed Nd:YAG or YLF lasers, which are specialized for the time-resolved PIV, have been available commercially. Doorne et al. (2003) have developed time-resolved stereoscopic PIV (TRSPIV) up to several hundreds Hz by using a Nd:YLF laser and CMOS cameras for the measurement of water flow turbulence in a pipe. To investigate turbulence characteristics in detail, however, higher spatial and temporal resolution up to several tens kHz is required. Especially, to understand the dynamics of vortical structure and its relations to turbulence statistics, sequential images of eddy motions with high temporal resolution are necessary. In our previous studies, we have developed TRSPIV up to 26.7kHz (Tanahashi et al., 2003; 2004a) by adopting Nd:YAG lasers for industrial processing and CMOS cameras.

Measurement methods of nine velocity gradient have also been developed to obtain more detailed flow properties. Kähler and Kompenhans (2000) first proposed dual-plane stereoscopic PIV (DPSPIV) (they called it multiple plane stereo PIV). They separated the scattering light from parallel laser sheets by using orthogonally polarized light sheets with polarizing beam-splitters. Hu et al. (2001) measured large-scale structure of a lobbed jet flow with DPSPIV by the same principle. The another way to separate the scattering light was proposed by Mullin and Dahm (2005). Instead of polarization, they used green and red light sheets with color filters. However, DPSPIV is limited to instantaneous measurement of nine velocity gradients and TRSPIV is limited to time-resolved measurement of three velocity components as described above. Both of PIV are not enough to measure dynamics of fine scale structure in turbulence.

In this study, time-resolved dual-plane stereoscopic PIV (TRDPSPIV), which provides all three velocity components and nine velocity gradients with high spatial and temporal resolutions, has been developed. Fine scale structure of turbulence was measured in a turbulent jet by the developed TRDPSPIV and the obtained results were compared with DNS in detail.

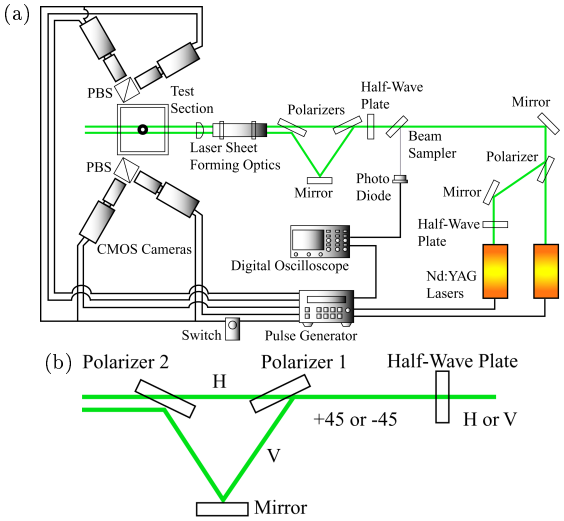

Figure 1: Schematic of time-resolved dual-plane stereoscopic PIV system (a) and parallel beam forming optics (b).

TIME-RESOLVED DUAL-PLANE STEREOSCOPIC PIV

System Setup

Figure 1 (a) shows a schematic of the time-resolved dual-plane stereoscopic PIV system. This system consists of two high-repetition-rate Nd:YAG lasers (Lee Laser, LDP-100MQG), several optics, four CMOS cameras (Vision Research, Phantom V7.1) and a pulse generator (LabSmith, LC880). The frequency of Nd:YAG lasers in conventional PIV has been no more than several tens Hz. However, in this system, we have adopted high power and high-repetition-rate pulse lasers for industrial processing as a light source. The maximum power of these lasers is 50W at 10kHz.

Laser beams from two lasers become doubled-pulsed beams through the laser beam combining optics which include a half-wave plate (CVI Laser) and a polarizer (CVI Laser), and each beam is divided into two parallel beams for dual-plane laser sheets through the parallel beam forming optics shown in Fig. 1(b). In Fig. 1 (b), H and V represent horizontal and vertical polarization, respectively. Polarization of each beam, which has horizontal or vertical polarization, rotates 45° through the half-wave plate, and each beam is divided into two beams at the first polarizer. One beam, which has horizontal polarization, passes through the first polarizer, and the other, which has vertical polarization, is reflected. Then, at the second polarizer, parallel beam is formed. The divided laser beams are expanded by sheet forming optics. After the illumination of the tracer particles with polarized laser beam, the polarizing beam splitter cube separates the incident wave-front scattered from the particles in two parts. The CMOS cameras are located with 18 degrees inclined forward with respect to normal to the measurement plane to capture forward scattered light. In this study, only using two Nd:YAG lasers, DPSPIV is realized by adopting the parallel beam forming optics. Note that most of DPSPIV systems require four lasers (Kähler and Kompenhans, 2000; Hu et al., 2001; Mullin and Dahm, 2005), except for Ganapathisubramani et al. (2005), in which a non-polarizing beam splitter is used to divide a beam.

The CMOS camera used in this study can record images with 512×256 pixels at 15.8kHz or 256×256 pixels at 26.7kHz. For the maximum resolution (800×600 pixels), this camera can record at 4.8kHz. The CMOS camera starts to expose 3μs after the trigger negative edge. Beams from each laser are synchronized to each frame interval. Repetition rates of two Nd:YAG lasers are a half of the camera frame rate respectively and velocity vectors are calculated from successive images by a cross correlation method. Generally, cameras need the dead time (T_S) to store data between camera frames and the time interval of successive images (Δt) is limited by this dead time. The theoretical minimum T_S of the CMOS camera used in this study is about 5μs. The images can be acquired with $\Delta t = 7\mu$s in our preliminary test, which means that this PIV system can be applicable to relatively high-speed flows.

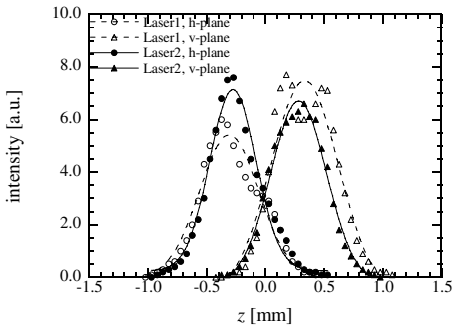

Figure 2: Intensity profile of the dual-plane laser sheets in the perspective direction at the center of the measurement region.

Characteristics of Dual-Plane Laser Sheets

In DPSPIV, it is important to estimate the distance between two measurement planes because the distance directly affects the results of velocity derivatives in the out-of-plane direction $\partial u_i/\partial z$. In addition, the parallelism also affects the accuracy for $\partial u_i/\partial z$, and the thicknesses determine the spatial resolution for the z direction. Mullin and Dahm (2005) measured these values by traversing a knife edge and detecting the transmitted light onto a photodiode. Ganapathisubramani et al. (2005) adopted the "burn method" to estimate them easily and roughly. In the present system, these values are measured by traversing a photodiode with a 10μm-pinhole across the laser sheets at 3×3 points with 5mm spacing in the traveling direction of the laser sheets and 3mm spacing in the direction normal to it.

Figure 2 shows one example of the intensity profiles of the dual-plane laser sheets for each laser with Gaussian fits. The laser sheets for two lasers with the same polarization coincide very well and have almost the same intensity. From the Gaussian fits of these profiles, the center of the laser sheets and the half value of the intensity are determined. These locations are plotted in Fig. 3. This figure also confirms the good agreement of the path of the two laser sheets. It is found that the laser-sheet thicknesses do not vary significantly through the measurement region because of the relatively long focal length (1000mm) of cylindrical lens for generating the waist. Since the distance between two laser sheets can be set arbitrarily within about 700μm by translating the second polarizer in the parallel beam forming optics, the laser sheets are aligned appropriately to prevent them from overlapping with each other.

Parallelism between the laser sheets is examined from the distribution of the center points in x and y directions. As a result, the divergence angle between two planes was less than 3.18mrad, which is enough for DPSPIV. To evaluate the error due to the scattering from other plane, polarized

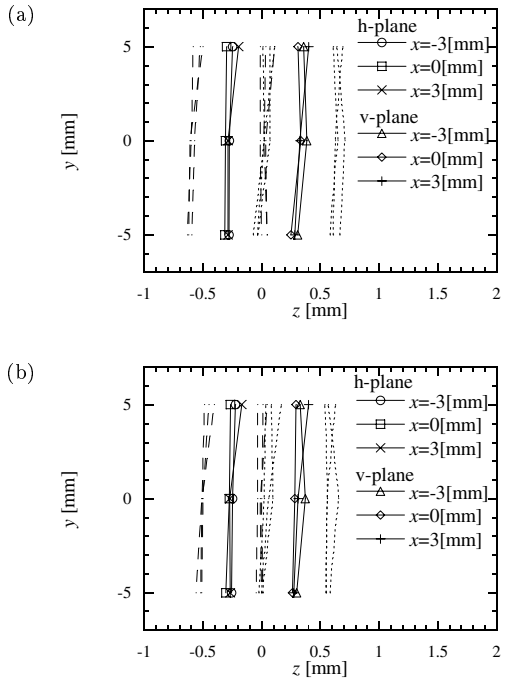

Figure 3: Distribution of the peak and half value of the laser intensity for laser 1 (a) and laser 2 (b). Solid lines represent the peak (i.e. the center of the laser sheets), and broken lines and dotted lines do the half value.

light intensities from single polarized laser beam exposure was measured. The error due to the scattering on the other plane is less than 3.5%.

Velocities and Gradients

In this study, high spatial resolution PIV algorithm developed by our previous study (Tanahashi, 2002) is used. To ensure the accuracy of the PIV measurement, the elimination scheme of the spurious vectors and noises is established by a PIV simulation based on DNS of particle-laden homogeneous isotropic turbulence. Note that number of the spurious vectors included in the raw data is very few (less than 0.5%) in the present measurements since the spatial resolution (size of the interrogation region) is nearly the same with that of DNS, and the elimination scheme is mainly used to cutoff the high-wave-number noises which exceed the spatial resolution of PIV. The high-wave-number noises are introduced by the overlap of the interrogation regions. From two-dimensional velocity fields obtained by each CMOS camera, three-component velocity vectors on a two-dimensional plane are calculated by using a geometrical relation (Willert, 1997; Prasad, 2000). As spurious vectors can not be completely eliminated by instantaneous velocity vectors, temporal cutoff filter, which is an advantage of the present time-resolved PIV, was also adopted at each velocity-defined point in the present work (Tanahashi, 2003; 2004a).

From the three component velocities in the dual planes, nine velocity gradients in the central plane between the dual planes are calculated. The velocities are linearly interpolated, and using the interpolated velocities, velocity gradients in the in-plane directions ($\partial u_i/\partial x$ and $\partial u_i/\partial y$) are derived by 4th order central finite difference scheme. Velocity gradients in the out-of-plane directions ($\partial u_i/\partial z$) are calculated by 2nd order central finite difference scheme using the velocities in the dual planes.

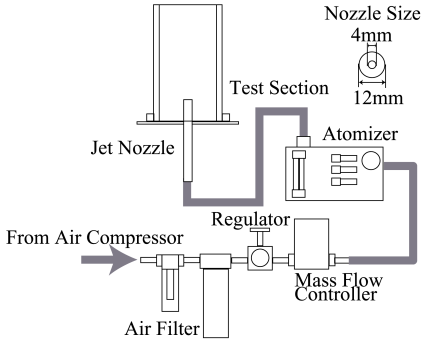

Figure 4: Experimental apparatus of a turbulent jet.

EXPERIMENTAL APPARATUS AND CONDITIONS

Figure 4 shows the experimental apparatus of a turbulent jet. Air from a compressor is regulated to a constant pressure and constant flow rate by pressure regulators and a digital mass flow controller, and is seeded with droplets generated by an atomizer (TSI, Six-Jet Atomizer, Model 9306). Then, the air is led to a nozzle to form a jet. In this study, DOS (dioctyl sebacate) was used as tracer particles (mean diameter is about 1μm). The orthogonal polarization is maintained by adopting liquid particles. The external and internal diameters of the nozzle are 12mm and 4mm, respectively. To prevent spreading of particles to circumference, the test section is surrounded by an acrylic duct with cross section of 32cm$\times$32cm.

In this study, measurement was carried out at $Re_D = 5316$ and $x/D = 60$, where Re_D is Reynolds number based on the nozzle diameter and mean axial velocity at the jet exit and x is distance from the jet exit. Preliminary measurements by a hotwire show that mean velocity $u_m = 1.63$m/s, r.m.s. of velocity fluctuation $u'_{rms} = 0.443$m/s, Taylor microscale $\lambda = 2.13$mm, Kolmogorov length $\eta = 137\mu$m, Kolmogorov velocity $u_k = 0.110$m/s, and Reynolds number based on Taylor microscale $Re_\lambda = 76.8$. Based on these statistics, the camera resolution was determined to be 512×256pixels for 8.0mm$\times$4.0mm region, which means that the spatial resolution of PIV is 2.7η (375μm) for 24×24pixels interrogation region. This spatial resolution is the same order of that of DNS of turbulent flows. Note that the velocity vectors are evaluated with 50% overlap. In this sense, velocity vectors are obtained every 1.35η. Frequency of four cameras is set to 15.8kHz and repetition rate of two Nd:YAG lasers is set to 7.9kHz, which results in 7.9kHz temporal resolution for the velocity measurement. Time interval between successive images (Δt) is set to 42μs. The FWHM (full width at half maximum) of laser sheet thickness is 618μm and 507μm for each lasers. The thickness of the laser sheet is measured by the photodiode scanning with a 10μm-pinhole as described above. The separation between two laser sheets is set to be 584μm (4.3η). The PIV measurement was conducted during about 7.5s in total.

PERFORMANCE OF TRDPSPIV

Figure 5 shows typical distributions of fluctuating velocity vectors and vorticity (ω_z) on the both planes with time interval 506μs. Here, white represents positive vorticity and black does negative one. The visualized distance between two measured planes is ten times the real scale for easy understanding. Since the measurement is conducted in fully

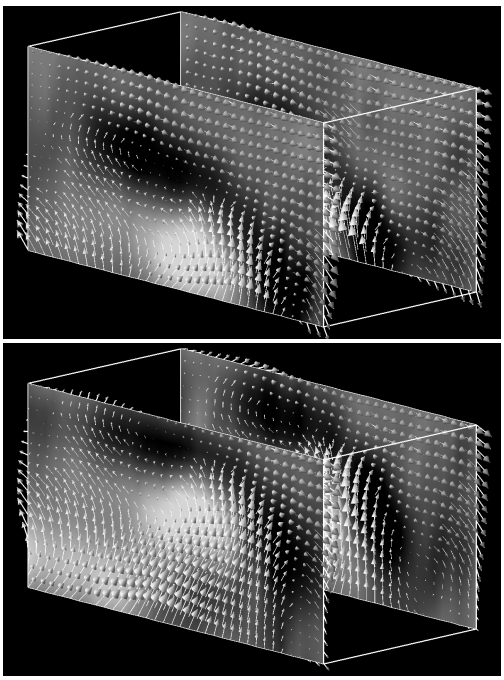

Figure 5: Typical velocity vectors and vorticity (ω_z) distributions with time interval 506μs.

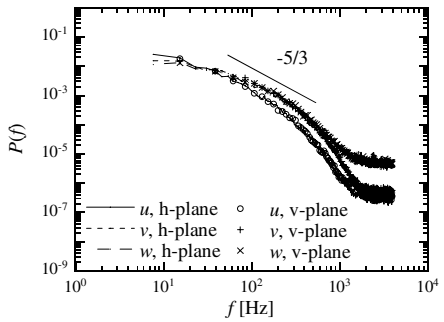

Figure 6: Power spectra of three velocity components at each polarization plane.

developed turbulent jet, fluctuations of velocities and vorticity are relatively high. As the distance between two planes is 4.3η, velocity and vorticity patterns are very similar in the both planes. The enough temporal resolution of the present PIV provides movies of fine scale motion in turbulence (not shown here).

As shown in our previous study (Tanahashi et al., 2004a), the time-resolved single-plane PIV can measure turbulent fluctuation which have an inertial subrange in power spectrum. In this study, power spectra of three velocity components in dual planes can be obtained simultaneously (Fig. 6). The power spectra of the same velocity component coincide very well. This result suggests that the fluctuation of velocities with small distance (4η) is measured accurately. Although the accuracy of the out-of-plane velocity component (w) is a little bit lower than that of other velocity components in high frequency range, it is enough in the inertial subrange.

Probability density functions of longitudinal and lateral velocity derivatives are shown in Fig. 7(a) and (b). The derivatives are normalized by their r.m.s. values. The results obtained from TRDPSPIV are compared with those from DNS of homogeneous isotropic turbulence with $Re_\lambda = 60.1$ and 97.1. The longitudinal and lateral velocity derivatives

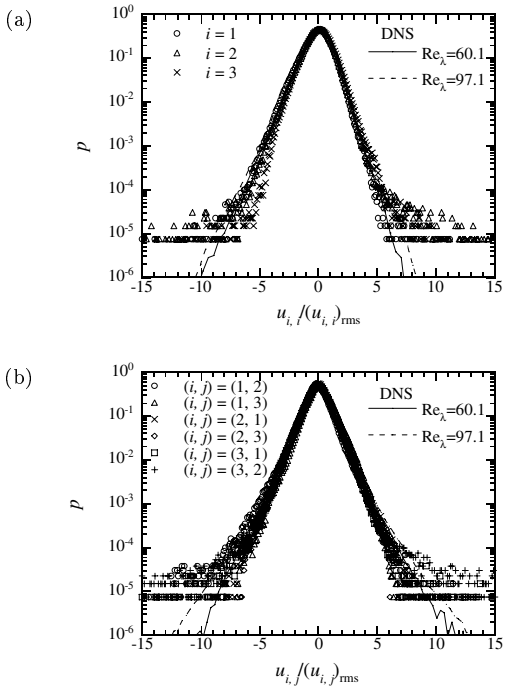

Figure 7: Probability density functions of longitudinal (a) and lateral (b) velocity derivatives.

by TRDPSPIV agree very well with those by DNS. The shape of probability density function, which is represented by skewness and flatness factors in general, is nearly the same with that obtained by DNS. These results show that TRDPSPIV gives all velocity gradients with enough accuracy.

From the nine-component velocity gradients obtained by the present PIV, vorticity vectors ω_i ($= \epsilon_{ijk}W_{jk}$), second invariant of velocity gradient tensor defined as

$$Q = -\frac{1}{2}(S_{ij}S_{ij} - W_{ij}W_{ij}) \tag{1}$$

and energy dissipation rate ε ($= 2\nu S_{ij}S_{ij}$) can be calculated exactly, where ϵ_{ijk} is Eddington's epsilon, and S_{ij} and W_{ij} denote symmetric and antisymmetric parts of the velocity gradient tensor A_{ij};

$$A_{ij} = S_{ij} + W_{ij}, \tag{2}$$

$$S_{ij} = \frac{1}{2}\left(\frac{\partial u_i}{\partial x_j} + \frac{\partial u_j}{\partial x_i}\right), \tag{3}$$

$$W_{ij} = \frac{1}{2}\left(\frac{\partial u_i}{\partial x_j} - \frac{\partial u_j}{\partial x_i}\right). \tag{4}$$

In the present study, ω_i and Q are used for identification of fine scale eddies in turbulence, which is discussed in the next section. η and u_k obtained from the preliminary measurements by a hotwire are estimated based on the assumption of isotropic and Taylor's hypothesis. On the other hand, since ε ($\bar{\varepsilon} = 4.85\mathrm{m}^2/\mathrm{s}^3$) is derived without any assumption from the present PIV, η ($= (\nu^3/\varepsilon)^{1/4}$) and u_k ($= (\varepsilon\nu)^{1/4}$) are calculated more precisely. The results obtained by the PIV are $\eta = 162\mu$m and $u_k = 9.23 \times 10^{-2}$m/s.

CHARACTERISTICS OF FINE SCALE EDDIES

To investigate scaling law of the coherent fine scale eddies, it is necessary to identify a method for extracting vortices from instantaneous turbulent flow field. The high

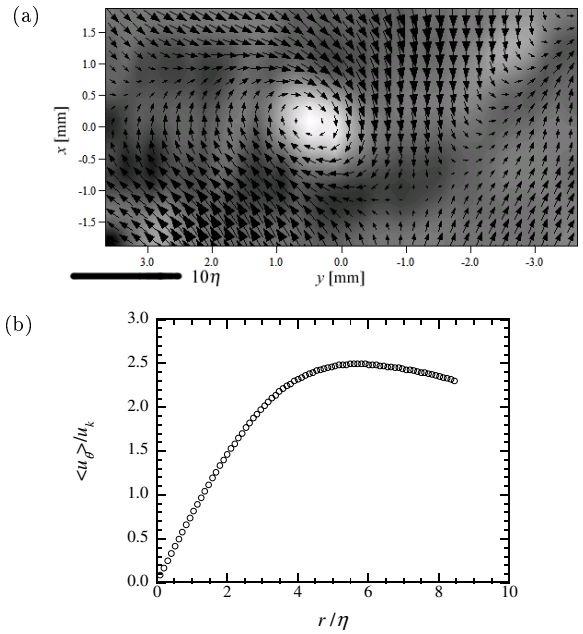

Figure 8: Distribution of second invariant and velocity vectors around the typical fine scale eddy (a) and distribution of mean azimuthal velocity of the typical fine scale eddy.

vorticity or enstrophy regions have been widely used to identify coherent structures and vortical structures (Hussain and Hayakawa, 1987; She et al., 1990; Jiménez and Wray, 1998). However, vorticity magnitude is not always appropriate method for identification of vortical structures, since high vorticity regions represent tube-like and sheet-like structures and they exist simultaneously in the flows with a background shear.

In our DNS studies (Tanahashi et al., 1997; 2001; 2004b), coherent fine scale eddies were educed without any threshold by using an identification scheme based on the local flow pattern. The identification scheme consists of the following steps:

- Evaluation of Q at each collocation point from the results of DNS.
- Probability of existence of positive maxima of Q near the collocation points is evaluated at each collocation point from the Q distribution. The case that a maximum of Q coincides with a collocation point is very rare, so it is necessary to define probability on collocation points.
- Collocation points with high possibility of existence are selected to survey actual maxima of Q. Locations of Q maxima are determined by applying a three dimensional fourth-order Lagrange interpolation to DNS data.
- At the maximum second invariant point, a horizontal plane perpendicular to the vorticity vector is defined and a cylindrical coordinate system with the maximum point as the origin is considered. The velocity vectors are projected on this coordinate and mean azimuthal velocity is calculated.
- A point that has minimum variance of azimuthal velocity is surveyed near the maximum point. In this process, cylindrical coordinate system is always renewed around a new searched point.

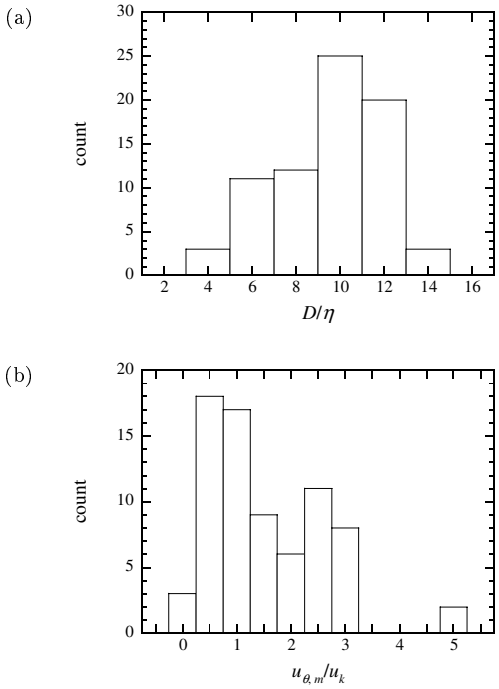

Figure 9: Histograms of diameter (a) and maximum azimuthal velocity (b) of the measured fine scale eddies.

- Statistical properties are calculated around the points.

From the distribution of Q, two-dimensional cross sections of the coherent fine scale eddies are identified by using this identification scheme. The educed section includes a local maximum of Q along the axis of a coherent fine scale eddy and a center point of swirling motion is identified. As for the present study, since measured velocities are limited to dual planes with small distance, another condition is added to the identification scheme. Eddies nearly perpendicular to the measurement planes are identified. As the spatial distribution of rotating axis of the fine scale eddy is random for fully-developed turbulent flow except for near wall turbulence (Tanahashi et al., 2001; 2004b), this additional condition does not affect the results.

Figure 8(a) shows a distribution of second invariant and velocity vectors around a typical fine scale eddy. The velocity at the center of the eddy is subtracted from the velocity field, and the color represents the second invariant. Here, white represents positive Q and black does negative one. The angle between the vorticity vector at the center of the eddy and the measurement planes is 87.3°. The asymmetric characteristic of the fine scale eddy shown in Fig. 8(a) agrees well with that obtained from DNS (Miyauchi et al., 2002; Kang et al., 2006). Figure 8(b) shows mean azimuthal velocity profile of the typical fine scale eddy. The radius and the mean azimuthal velocity in Fig. 8(b) are normalized by η and u_k which are obtained from the present PIV. The diameter (D) of the fine scale eddy is defined as the distance between the center and the locations where the mean azimuthal velocity shows the maximum or minimum value. The diameter of this eddy is 11.4η and the maximum azimuthal velocity ($u_{\theta,max}$) is $2.5u_k$.

Figure 9 shows the histograms of the diameter and maximum azimuthal velocity of the fine scale eddies. The diameter and maximum azimuthal velocity are normalized by η and u_k calculated from the PIV data. Because of the limitation of the relatively small measurement region, diameter

for an identifying eddy is set to less than 16η, and eddies larger than 16η are not counted in these histograms. The number of educed fine scale eddies from the above identification scheme was 74 on condition that the angles between eddies and the measurement planes are 80 to 90 degrees. The histograms of the diameter and maximum azimuthal velocity show peaks at $D/\eta \approx 10$ and $u_{\theta,max}/u_k \approx 0.75$. It should be noted that the actual peak of D might be lower than the present results because the somewhat tilted cross section of the eddies are detected in this study. In our DNS studies (Tanahashi et al., 1997; 2001; 2004b), it is shown that the most expected diameter and maximum azimuthal velocity are 8η and $1.2u_k$. The characteristics of the fine scale eddies obtained in the present study are very similar to those of coherent fine scale eddy which has been shown by detailed analyses of DNS, which gives experimental support for the existence of the coherent fine scale eddy in turbulence. However, since the number of educed eddies, which is 74, is insufficient in quantity, statistically-meaningful data is needed to ensure this suggestion in the future work.

CONCLUSIONS

In this study, time-resolved dual-plane stereoscopic PIV has been developed, and fine scale structure of turbulence was measured in a turbulent jet.

Three velocity components and nine velocity gradients are measured with nearly the same accuracy as DNS by the time-resolved dual-plane stereoscopic PIV. It is shown that probability density functions of the measured nine velocity gradients agree well with those obtained from DNS.

Coherent fine scale eddies can be identified by the time-resolved dual-plane stereoscopic PIV using the identification scheme developed in our DNS studies. The detected fine scale eddies have asymmetric characteristics, and the histograms of the diameter and maximum azimuthal velocity show peaks at $D/\eta \approx 10$ and $u_{\theta,max}/u_k \approx 0.75$. These characteristics are very similar to those obtained from detailed analyses of DNS.

REFERENCES

van Doorne C. W. H., Hof, B., Lindken, R. H., Westerweel, J., and Dierksheide, U., 2003, "Time Resolved Stereoscopic PIV in Pipe Flow. Visualizing 3D Flow Structures", *Proceedings of 5th International Symposium on PIV.*

Ganapathisubramani, B., Longmire, E. K., Marusic, I., and Pothos, S., 2005, "Dual-Plane PIV Technique to Determine the Complete Velocity Gradient Tensor in a Turbulent Boundary Layer", *Experiments in Fluids*, Vol. 39, pp. 222-231.

Hu, H., Saga, T., Kobayashi, T., Taniguchi, N., and Yasuki, M., 2001, "Dual-Plane Stereoscopic Particle Image Velocimetry: System Set-up and its Application on a Lobed Jet Mixing Flow", *Experiments in Fluids*, Vol. 31, pp. 277-293.

Hussain, A. K. M. F., and Hayakawa, M., 1987, "Eduction of Largescale Organized Structure in a Turbulent Plane Wake", *Journal of Fluid Mechanics*, Vol. 180, pp. 193-229.

Jiménez, J., and Wray, A. A., 1998, "On the Characteristics of Vortex Filaments in Isotropic Turbulence", *Journal of Fluid Mechanics*, Vol. 373, pp. 255-285.

Kähler, C. J., and Kompenhans, J., 2000, "Fundamentals of Multiple Plane Stereo Particle Image Velocimetry", *Experiments in Fluids*, Vol. 29, pp. 70-77.

Kang, S.-J., Tanahashi, M., and Miyauchi, T., 2006, "Elliptic Feature of Coherent Fine Scale Eddies in Turbulent Channel Flows", *Journal of Mechanical Science and Technology*, Vol. 20, pp. 262-270.

Miyauchi, T. et al., 2002, "Scalar Dissipation Rate and Coherent Fine Scale Eddies in Turbulence", *Proceedings of International Symposium on Dynamics and Statistics of Coherent Structure in Turbulence*, p. 249.

Mullin, J. A., and Dahm, W. J. A., 2005, "Dual-Plane Stereo Particle Image Velocimetry (DSPIV) for Measuring Velocity Gradient Fields at Intermediate and Small Scales of Turbulent Flows", *Experiments in Fluids*, Vol. 38, pp. 185-196.

Prasad, A. K., 2000, "Stereoscopic Particle Image Velocimetry", *Experiments in Fluids*, Vol. 29, pp. 103-116.

She, Z. S., Jackson, E., and Orszag, S. A., 1990, "Intermittent Vortex Structures in Homogeneous Isotropic Turbulence", *Nature* Vol. 344, pp. 226-228.

Tanahashi, M., Miyauchi, T., and Ikeda, J., 1997, "Identification of Coherent Fine Scale Structure in Turbulence", *IUTAM Symposium. Simulation and Identification of Organized Structures in Flows.*, pp. 131-140.

Tanahashi, M., Iwase, S., Uddin, Md. A., and Miyauchi, T., 1999, "Three-Dimensional Features of Coherent Fine Scale Eddies in Turbulence", *Proceedings 1st International Symposium on Turbulence and Shear Flow Phenomena, Begell House Inc.*, pp. 79-84.

Tanahashi, M., Iwase, S., and Miyauchi, T., 2001, "Appearance and Alignment with Strain Rate of Coherent Fine Scale Eddies in Turbulent Mixing Layer", *Journal of Turbulence*, Vol. 2, pn. 6.

Tanahashi, M., Ootsu, M., Fukushima, M., and Miyauchi, T., 2002, "Measurement of Coherent Fine Scale Eddies in Turbulent Mixing Layer by DPIV", *Engineering Turbulence Modeling and Measurements*, Vol. 5 p. 525.

Tanahashi, M., Fukuchi, Y., Choi, G.-M., Fukuzato, K., and Miyauchi, T., 2003, "High Spatial Resolution Time-Series PIV for Turbulence Measurement", *Proceedings of 4th International Symposium on Turbulence, Heat and Mass Transfer*, pp. 245-252.

Tanahashi, M., Kang, S.-J., Miyamoto, T., Shiokawa, S., and Miyauchi, T., 2004a, "Scaling Law of Fine Scale Eddies in Turbulent Channel Flows up to $Re_\tau = 800$", *International Journal of Heat and Fluid Flow*, Vol. 25 pp. 331-340.

Tanahashi, M., Fukuchi, Y., Choi, G.-M., Fukuzato, K., and Miyauchi, T., 2004b, "The Time-Resolved Stereoscopic Digital Particle Image Velocimetry up to 26.7 kHz", *Proceedings of 12th International Symposium on Applications of Laser Techniques to Fluid Mechanics.*

Upatnieks, A., Driscoll, J. F., and Ceccio, S. L., 2002, "Cinema Particle Imaging Velocimetry Time History of the Propagation Velocity of the Base of a Lifted Turbulent Jet Flame", *Proceedings of Combustion Institute*, Vol. 29, pp. 1897-1903.

Vogel, A., and Lauterborn, W., 1988, "Time Resolved Particle Image Velocimetry", *Optics and Lasers in Engineering*, Vol. 9, pp. 277-294.

Willert, C., 1997, "Stereoscopic Digital Particle Image Velocimetry for Application in Wind Tunnel Flows", *Measurement Science and Technology*, Vol. 8, pp. 1465-1479.